Gas-Phase Processes

International Edition: DOI: 10.1002/anie.201500649
German Edition: DOI: 10.1002/ange.201500649

Doping Effects in Cluster-Mediated Bond Activation

*Helmut Schwarz**

bond activation · oxide clusters · doping · gas-phase processes · reaction mechanisms

Dedicated to Professor Jürgen Troe

Gas-phase investigations of judiciously doped oxide clusters permit to address fundamental challenges related to, for example, the low-temperature oxidation of CO or the selective conversion of hydrocarbons. Modifying the size and composition of a free cluster in a controlled way enables the modification of local charge effects and of spin states, and spectroscopic studies in combination with computational work help to identify the active site of a catalyst and to unravel mechanistic details. Also, the interplay of the support material with the reactive part of a composite catalyst cluster can be addressed. Examples will be presented demonstrating how and why the gas-phase reactivities of heteronuclear clusters, in comparison with their homonuclear counterparts, toward small, generally rather inert molecules can be increased, decreased, or not significantly affected.

1. Introduction

The ultimate goal in heterogeneous catalysis is to make use of each and every atom of supported (metal) catalysts, that is, in the extreme to perform single-atom catalysis (SAC). While this task constitutes a nontrivial challenge in "real-life" chemistry,[1] in the gas-phase SAC can be achieved in a rather straightforward manner by conducting experiments with mass-selected species under (near) single-collision conditions.[2–5] In fact, gas-phase studies on "isolated" reactants provide an ideal arena for probing experimentally the energetics and kinetics of a chemical reaction in an unperturbed environment at a strictly molecular level, without being obscured by difficult-to-control or poorly defined solvation, aggregation, counter ions, and other effects. Thus, they offer an opportunity to explore the concept of SAC or, more generally, to help in identifying the active site(s) of single-site catalysts directly; the latter constitutes one of the intellectual cornerstones in contemporary catalysis.[6–8] In addition, in gas-phase experiments, reactions can be analyzed in detail, mechanisms uncovered, and questions can be addressed on how factors such as cluster size and dimensionality, stoichiometry, oxidation number, spin and charge states, degree of coordinative saturation etc. will affect the outcome of a chemical process.[5,9,10] While this approach, on principal ground, never accounts for all the details that prevail at a surface or in solution, when complemented by appropriate computational or spectroscopic studies, investigations in the gas phase have proved extremely meaningful over the last two decades, because they provide a systematic approach to address the above-mentioned questions, and, moreover, offer a conceptual framework. This has been demonstrated, for example, for the DEGUSSA process, that is, the large-scale, platinum-mediated coupling of CH_4 and NH_3 to generate HCN. Crucial insight on the elementary steps and on how to improve the catalytic performance were derived initially from mass-spectrometry-based studies;[11,12] later, these predictions were confirmed by in situ photoionization experiments.[13] Quite clearly, each and every piece of information that helps to optimize or improve the often trial-and-error-based strategies of catalyst developments[8,10] is highly welcome.

An important aspect that supports the feasibility of using small systems as catalytic models derives from the fact that chemistry is a *local* event: bond breaking and bond making are confined to the catalytically active site(s). Consequently, studying the chemistry and physics of free clusters has become extremely helpful in uncovering many facets of quite a few heterogeneously catalyzed processes.[2–5,9,10,14,15] Of particular interest are those systems in which size and doping effects control the reaction. The properties of clusters change dramatically as a function of size, one atom at a time, or are affected by the implementation of a different element; in short: Each atom counts![3,16] Too many examples exist to provide a comprehensive account on, for example, the power of micro- and nanoalloys[17] in real-life catalysis; therefore, it may suffice to mention just four systems:

1) A single platinum atom anchored to the surface of iron oxide mediates efficient oxidation of CO.[18]

[*] Prof. Dr. H. Schwarz
Institut für Chemie, Technische Universität Berlin
Straße des 17. Juni 115, 10623 Berlin (Germany)
E-mail: helmut.schwarz@tu-berlin.de

© 2015 Wiley-VCH Verlag GmbH & Co. KGaA, Weinheim

2) The active site in the heterogeneously catalyzed industrial methanol synthesis consists of Cu steps decorated with Zn atoms.[19]
3) It is a Zn-doped zeolite that enables direct coupling of CH_4 and CO_2 to form acetic acid.[20]
4) The remarkable synthesis of hydrogen peroxide from O_2 and H_2 has been achieved by a binary Au–Pd catalyst.[21]

Not surprisingly, doped clusters in the gas phase—the chemistry of which forms the subject of this Review—also exhibit quite extraordinary features. For example, the $[PtZnH_5]^-$ cluster anion possesses an unprecedented planar pentagonal coordination for platinum and exhibits σ-aromatic character,[22] or the heterolytic cleavage of H_2, according to Eq. (1), is quite unique,[23] because the gold-free homonuclear cluster ion $[CeO_2]^+$ is not capable to thermally activate H_2.[23,24] As shown by DFT calculations, the gold atom of $[AuCeO_2]^+$ fulfils two functions, that is, it serves as the adsorption site for H_2 and facilitates the reaction.[23]

$$[AuCeO_2]^+ + H_2 \rightarrow [CeO_2H]^+ + AuH \quad (1)$$

One of the earliest examples for a gas-phase "microalloy catalysis" concerns the coupling of methane and NH_3 to generate HCN [Eq. (2)].[11] While platinum is crucial to activate methane and to initially form a platinum–carbene complex,[9,25,26] the presence of a coinage metal M (M = Cu, Ag, Au) is essential for the actual coupling of the carbene fragment with ammonia, as shown by experimental and relativistic DFT studies.[12,27–31] As depicted in Figure 1, none of the homonuclear cluster ions $[MM]^+$ (M = Cu, Ag, Au, Pt) mediates the C–N coupling. They are either unreactive with CH_4 (M = Cu, Ag, Au) or the carbene complex $[Pt_2(CH_2)]^+$ forms a carbide in the reaction with NH_3, rather than delivering C–N coupling products.

$$CH_4 + NH_3 \xrightarrow{\text{Pt alloy}} HCN + 3\,H_2 \quad (2)$$

In this Minireview, I will focus on two types of reactions by "doped" cluster ions, that is, 1) oxidation of CO under ambient conditions, and 2) the competition between hydrogen-atom transfer to the cluster or oxygen-atom delivery to hydrocarbons. While I will address questions related to, for example, the role of charge and spin states, the nature of the active site in the cluster, or discuss mechanistic features, I will refrain from describing any experimental or computational details, as these can be found in the original articles. Also, gas-phase spectroscopic studies of cluster ions conducted in the context of selective bond activation[26,32–35] will not be discussed in detail; rather, one system may suffice to illustrate the power of these techniques when combined with computational work.

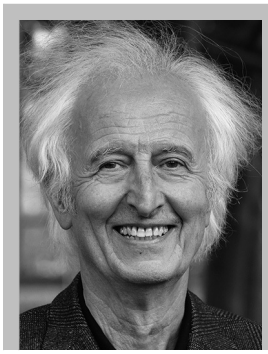

Helmut Schwarz is a Professor of Chemistry at the Technische Universität Berlin. Since 2008, he serves as President of the Alexander von Humboldt-Stiftung. In the course of his academic career, Dr. Schwarz has occupied visiting positions at 15 research institutions worldwide, has delivered more than 1000 invited or name lectures and published more than 950 peer-reviewed articles dealing with various aspects of gas-phase chemistry and physics.

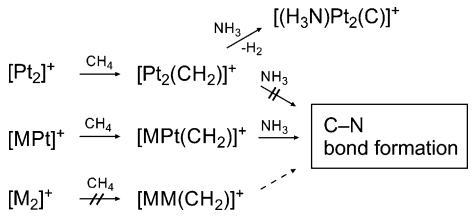

Figure 1. Activation of methane, coupling with ammonia, or carbide formation as a function of cluster composition with M = Cu, Ag, Au.

The homonuclear cluster oxide $[V_2O_4]^{\bullet+}$ exhibits no or only minor reactivity toward small hydrocarbons, such as CH_4, C_2H_6, C_3H_8, *n*-C_4H_{10}, and C_2H_4;[36] however, substitution of one vanadium atom by a phosphorus atom results in the highly reactive oxide $[VPO_4]^{\bullet+}$ (**1**), and this cluster leads to the oxidative dehydrogenation of and hydride abstraction from saturated alkanes as well as the conversion of C_2H_4 to CH_3CHO under thermal conditions.[37] The infrared photodissociation (IRPD) spectrum of $[VPO_4]^{\bullet+}$ (Figure 2) together with electronic structure calculations show the origin of this distinctly different behavior and, in addition, uncovers crucial mechanistic aspects. In $[V_2O_4]^{\bullet+}$, the unpaired electron is centered at one vanadium atom, thus corresponding to a mixed-valence cluster $[V^{IV}V^{V}O_4]^{\bullet+}$. In contrast to the structurally related $[V_2O_4]^{\bullet+}$ ion,[37,38] in the heteronuclear cluster **1** the reactive site is located at the P–O unit, and the reactions are driven by the favored reduction process $P^{+V} \rightarrow P^{+III}$ (for the conversion $C_2H_4 \rightarrow CH_3CHO$) and the fact that the phosphorus atom is a better hydride acceptor compared to the vanadium atom. Isomers **2** and **3** of $[VPO_4]^{\bullet+}$ are much too high in energy to play a role and, as shown in Figure 2, they are not generated in the experiment.

2. Oxidation of CO under Ambient Conditions

Arguably, the metal-mediated $CO \rightarrow CO_2$ conversion is one of the most often studied systems, both at surfaces[39] and in the gas phase.[40] In recent years, the focus of interest shifted from the investigation of homonuclear to "doped" clusters, as it turned out that even seemingly simple phenomena, such as adsorption energies, dissociative versus physical adsorption, and cluster reorganization or cluster fragmentation upon landing of CO, crucially depend on the composition of the heteronuclear clusters.[41–44] In this chapter, I will primarily discuss mechanistic aspects of the redox process mediated by heteronuclear metal oxides (for an exhaustive review on homonuclear cluster oxides, see Ref. [40]).

The couple $[AlVO_3]^{\bullet+}/[AlVO_4]^{\bullet+}$ serves as an example for probing the catalytic redox features and determining the active site of a heteronuclear metal-oxide cluster in the room-temperature oxidation of CO by N_2O.[45] In the presence of CO (Figure 3), $[AlVO_4]^{\bullet+}$ is reduced to $[AlVO_3]^{\bullet+}$, and if N_2O

 © 2015 Wiley-VCH Verlag GmbH & Co. KGaA, Weinheim

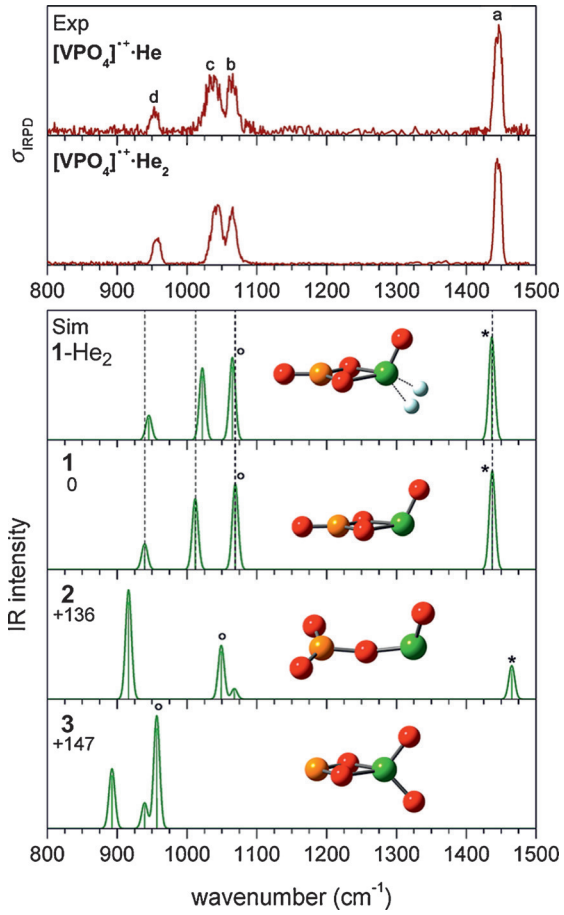

Figure 2. Experimental IRPD spectra (top) of the helium complexes $[VPO_4]^{+}\cdot He_{1,2}$ compared to simulated B3LYP + D/TZVPP linear absorption spectra of three bare isomers (**1**–**3**) and the helium-tagged isomer **1**-He_2. Given values indicate the zero-point-corrected relative energies (in kJ mol^{-1}) of the optimized structures (yellow P; green V; red O; gray He). The V=O stretching modes are marked with a circle, and P=O modes with an asterisk (adapted from Ref. [37]).

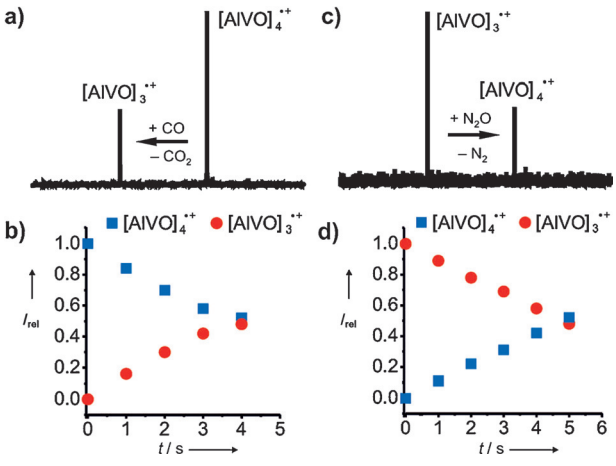

Figure 3. Fourier-transform ion-cyclotron resonance (FT-ICR) mass spectra showing the thermal reactions of a) $[AlVO_4]^{+}$ with CO ($t = 3$ s) and c) $[AlVO_3]^{+}$ with N_2O ($t = 2$ s). The relative intensities of $[AlVO_4]^{+}$ and $[AlVO_3]^{+}$ with increasing reaction times are shown in (b) and (d), respectively (adapted from Ref. [45]).

is added, the reverse reaction occurs. Both processes are clean and proceed with efficiencies of 59 % and 65 % relative to the collision rate, respectively. In principle, the turnover number of the catalytic cycle is infinite.

DFT calculations provide insight into the actual mechanism and, in particular, the question of the active site in $[AlVO_4]^{+}$.[45] As shown in Figure 4, the transition state TS1 of

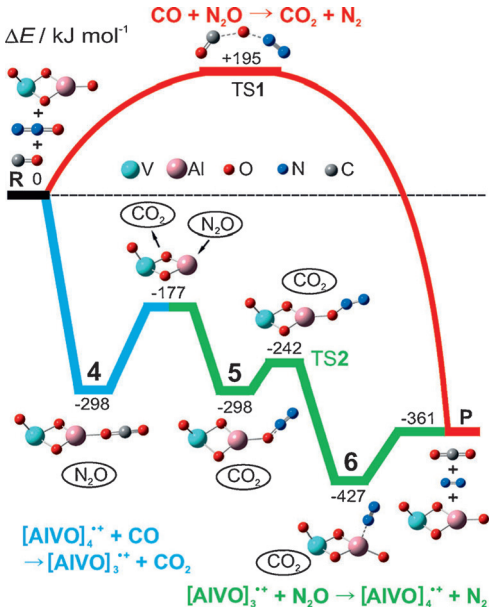

Figure 4. Potential-energy surfaces (B3LYP/TZVP) for the oxidation of CO by N_2O in the absence (red graph) and the presence of $[AlVO_4]^{+}$ (blue/green graphs). The relative energies ΔE are corrected for zero-point energy. The blue and green profiles correspond to the reaction of $[AlVO_4]^{+}$ with CO and of $[AlVO_3]^{+}$ with N_2O, respectively. TS = transition state; R = reactants = CO + N_2O + $[AlVO_4]^{+}$; P = product = CO_2 + N_2 + $[AlVO_4]^{+}$ (adapted from Ref. [45]).

the uncatalyzed reaction is much too high in energy to play a role under ambient conditions. In contrast, the catalytic conversion, which takes place at the doublet ground state of $[AlVO_4]^{+}$, commences by a barrier-free binding of the carbon atom of CO to the radical oxygen atom of the Al–$O_t^{\bullet}$ (O_t = terminal oxygen atom) moiety to generate intermediate **4**. This species is formed with an internal energy of 298 kJ mol^{-1} below the entrance channel; as the energy in an "isolated" system cannot be dissipated to a heat bath, the liberation of CO_2 (from "hot" **4**) occurs spontaneously, requiring only 121 kJ mol^{-1}. The catalytic cycle is completed by a straightforward, barrier-free reoxidation of $[AlVO_3]^{+}$ with N_2O.

Interestingly, this catalytic cycle of a redox couple cannot be promoted by the nonradical terminal oxygen atom of the V=O_t moiety of $[AlVO_4]^{+}$. Computational findings demonstrate that this pathway is kinetically and thermodynamically much less favorable than the one commencing at the Al–$O_t^{\bullet}$ unit (Figure 5). Thus, the existence and operation of an active site can even be probed in a rather small heteronuclear cluster.

A comparison of the reactivities of the heteronuclear couple $[AlVO_4]^{+}$/$[AlVO_3]^{+}$ and the homonuclear analogue

© 2015 Wiley-VCH Verlag GmbH & Co. KGaA, Weinheim

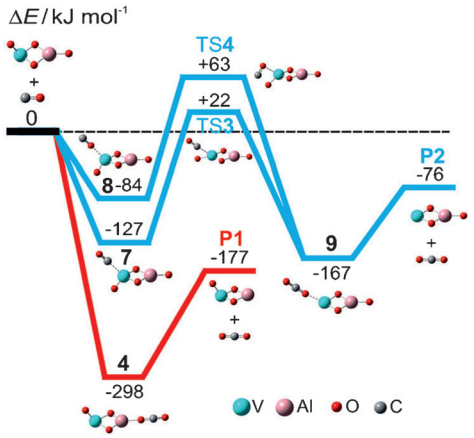

Figure 5. The reaction $[O_tV(\mu\text{-}O)_2AlO_t]^{\bullet+} + CO \rightarrow [V(\mu\text{-}O)_2AlO_t]^{\bullet+} + CO_2$ (blue lines) is kinetically inhibited and thermodynamically much less favorable than the process $[O_tV(\mu\text{-}O)_2AlO_t]^{\bullet+} + CO \rightarrow [O_tV\text{-}(\mu\text{-}O)_2Al]^{\bullet+} + CO_2$ (red line) (adapted from Ref. [45]).

$[Al_2O_3]^{\bullet+}/[Al_2O_2]^{\bullet+}$ shows that the superior performance of the bimetallic system derives from the fact that replacement of an Al atom by a V=O$_t$ unit totally inhibits the unwanted cluster fragmentation to generate Al^+ in the reaction of $[Al_2O_3]^{\bullet+}$ with CO.[46]

However, "doping" a cluster does not necessarily improve its catalytic performance. For example, all steps in the cycles shown in Figure 6 are highly exothermic; yet, kinetic barriers

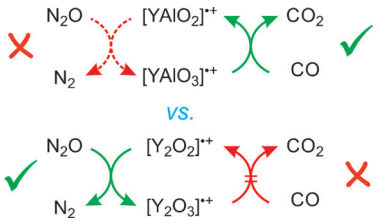

Figure 6. Bottlenecks in the cluster-mediated redox process $CO + N_2O \rightarrow CO_2 + N_2$.

impede efficient redox cycles.[47] While oxidation with N_2O corresponds to the bottleneck for the $[YAlO_2]^{\bullet+}/N_2O/CO$ system, oxidation of $[Y_2O_2]^{\bullet+}$ with N_2O is facile, but reduction of $[Y_2O_3]^{\bullet+}$ by CO is prevented on the ground that this cluster lacks a high-spin density at a terminal oxygen atom as present in $[YAlO_3]^{\bullet+}$. Rather, the unpaired electron is delocalized equally over two of the bridging yttrium atoms of $[Y_2O_3]^{\bullet+}$, and the absence of a "prepared state"[48] is the origin of the energy barrier for the OAT.

The role of the overall charge state of cluster oxides in the context of CO/N_2O conversion has been studied by the groups of Castleman and Bonačić-Koutecký.[14,49–51] Stoichiometric cluster oxides $[ZrO_2]_n^{\bullet+}$ and $[Zr_nO_{2n+1}]^{\bullet-}$ $(n = 1–4)$ have been generated and found to initiate oxidation of CO. While both the cations and anions possess terminal radical oxygen centers, at which the reaction commences, the cations are more reactive, thus suggesting that the charge state matters in the initial phase of generating the encounter complexes with CO. Furthermore, based on a theoretical analysis, it was proposed that by "doping" the charged zirconium oxides, for example, $[Zr_2O_4]^{\bullet+}$ or $[Zr_2O_5]^{\bullet-}$, with a metal that contains one electron more or less (i.e. Sc or Y), the generation of *neutral* bimetallic oxide clusters containing reactive M–O$_t$ centers should be feasible.[51] As indicated by DFT calculations, these systems (Figure 7) should undergo selective conversion of CO/N_2O in fully catalytic cycles under ambient conditions.

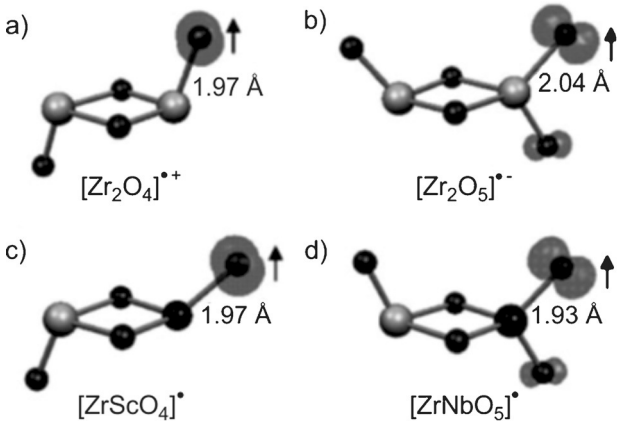

Figure 7. Calculated lowest-energy structures for a) $[Zr_2O_4]^{\bullet+}$, b) $[Zr_2O_5]^{\bullet-}$, c) $[ZrScO_4]^{\bullet}$, and d) $[ZrNbO_5]^{\bullet}$. The radical oxygen centers are indicated by an arrow, and the isosurfaces represent localized spin densities (adapted from Ref. [51]).

The landmark discovery of Haruta et al. that gold nanoparticles promote the low-temperature oxidation of CO[52] has triggered an avalanche of experimental and theoretical studies to address questions as the effect of particle size, the coordination number or the oxidation state of gold, the roles of support materials and support effects, etc.[53] Many of these and other questions have also been addressed in gas-phase experiments on free gold clusters, and the results have been reviewed repeatedly.[3,5,10,14,54,55] Here, I will briefly mention the remarkable effects of a single gold atom attached to three different metal-oxide cluster ions, as studied experimentally and computationally by He and co-workers.[56–58]

CO oxidation according to Eq. (3) proceeds with an efficiency of 23% relative to the collision rate.[56] Based on DFT calculations, the CO molecule is first attached to the loosely bound gold atom (Figure 8). CO oxidation without the direct participation of gold in $[AuFeO_3]^-$ or in gold-free $[FeO_3]^{\bullet-}$ can be ruled out on energetic grounds. In the course of the reaction, there is an electron flow such that the initially, nearly neutral gold atom delivers electrons to the FeO_3 unit upon forming an Au–C bond. In the subsequent oxidation of CO, the gold-atom transfers its CO ligand to the nearby "lattice" oxygen to form intermediate I2, in which the gold atom has accumulated a negative charge. This mechanism lends support to an Au-assisted Mars-van-Krevelen mechanism, as suggested to be operative in both the condensed[59,60] and the gas phase.[57] In addition, these gas-phase studies underline the crucial role that structural flexibility of the active site plays in catalytic processes, as well as the capability

 © 2015 Wiley-VCH Verlag GmbH & Co. KGaA, Weinheim

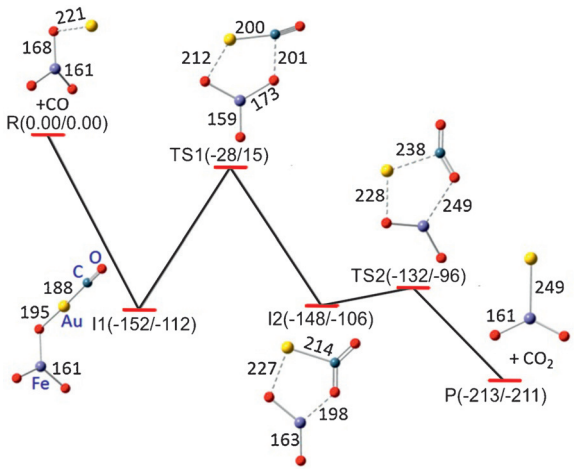

Figure 8. DFT-calculated potential-energy profile for the reaction $[AuFeO_3]^- + CO \rightarrow [AuFeO_2]^- + CO_2$. The zero-point-corrected energies and the Gibbs free energies at 298 K ($\Delta H_{0K}/\Delta G_{298K}$ in kJ mol^{-1}) are given with respect to the separated reactants. Bond lengths in pm (adapted from Ref. [56]).

of gold to serve as an electron-relay station by varying its charge and oxidation states as a response to the chemical environment. The latter feature is an immediate consequence of strong relativistic effects, which are responsible for much of the remarkable chemistry of gold.[61,62]

$$[AuFeO_3]^- + CO \rightarrow [AuFeO_2]^- + CO_2 \quad (3)$$

In the rather efficient reactions of Au-doped aluminum oxide clusters with CO and O_2, Figure 9, the oxidation catalysis is also driven by electron cycling primarily through making and breaking a Au–Al bond. As shown computationally, some of the species involved in the catalytic cycle exhibit quite unique bonding features. For example, the cluster intermediate $[AuAl_3O_4]^{\bullet+}$ contains both a reductive Au–Al bond and a highly oxidative $O^{\bullet+}$ radical center. In the $[AuAl_3O_n]^{\bullet+}$ system ($n = 3$, 4, 5) there is also a dramatic change in the charge of the gold atom along the reaction path; again, this is due to relativistic effects, which are also the cause for the significant differences of the Au–Al bond strength in $[AuAlO_4]^{\bullet+}$ and $[AuAlO_5]^{\bullet+}$. This [Au,Al,O] bimetallic system seems to be the first example of thermal catalytic CO oxidations by molecular oxygen mediated by a gas-phase cluster with a single gold atom acting as the active site.

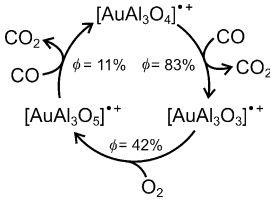

Figure 9. Catalytic oxidation of CO by O_2. Efficiencies (ϕ) are given relative to the collision rate (adapted from Ref. [58]).

3. How to Control Competitive Oxygen- versus Hydrogen-Atom Transfer?

As the gas-phase reactions of hydrocarbons with homonuclear metal-oxide clusters are well documented,[3–9,14,25,63–68] in this chapter the focus will be on presenting and discussing the often dramatic effects that "doping" exerts on these reactions.[69,70] I first mention the industrially relevant direct $CH_4 \rightarrow CH_2O$ conversion. While this process can be initiated at room temperature with the homonuclear oxides $[PtO_2]^{\bullet+}$,[71] $[CrO_2]^{\bullet+}$,[72] $[Al_2O_3]^{\bullet+}$,[73] or $[ReO_4]^+$,[74] the chemoselectivities and efficiencies are often disappointingly poor, and for the couple $[Y_2O_3]^{\bullet+}/CH_4$, one does not even observe any activation of methane.[75,76] The situation changes completely for the heteronuclear oxide $[YAlO_3]^{\bullet+}$ in that this cluster is both more reactive than $[Y_2O_3]^{\bullet+}$, and more selective than $[Al_2O_3]^{\bullet+}$ in its thermal reaction with CH_4.[77] Also, adding a single platinum atom to the $[Al_2O_4]^{\bullet-}$ cluster anion exerts a dramatic effect, and the oxidation of CH_4 in Eq. (4) occurs with an efficiency of 7%.[78a]

$$[PtAl_2O_4]^{\bullet-} + CH_4 \rightarrow [PtAl_2O_3H_2]^{\bullet-} + CH_2O \quad (4)$$

A computational analysis of Eq. (4) shows an extraordinary co-operative effect. The reaction is initiated by a Pt-mediated C–H bond activation, however, the support cluster $[Al_2O_4]^{\bullet-}$ does not act as an innocent spectator. Rather, as other oxygen-rich species,[70,79,80] its $O^{\bullet-}$ center abstracts a hydrogen atom from the oxygen-anchored CH_3 group to pave the way for eventually liberating CH_2O.[78]

3.1 Structural Effects on Hydrogen-Atom Transfer

The network of possible metal-oxide-mediated oxidations of hydrocarbons is depicted in Figure 10.[81] In the following, I begin with a discussion of the HAT reactions. Refs. [68–70] provide reviews on gas-phase aspects of this fundamental process, in particular of the role of unpaired spin densities at oxygen atoms to initiate a homolytic scission of the C–H bond at room temperature, Eq. (5). For $R = CH_3$, this cleavage is considered to correspond to the first and crucial step for the metal-oxide-mediated oxidative coupling of methane, Eq. (6).[82]

$$MO^{\bullet} + RH \rightarrow MOH + R^{\bullet} \quad (5)$$

$$2\,CH_4 + {}^1/_2\,O_2 \rightarrow C_2H_6 + H_2O \quad (6)$$

For alternative mechanistic views, in particular the possibility of a heterolytic activation of the C–H bond of methane at MgO surfaces or in Zn-doped zeolites, see Ref. [83] and [84]. As to the general features of an efficient metal-oxide-mediated gas-phase HAT from hydrocarbons, the consensus views can be summarized as follows:[68]

1) The presence of unpaired, high spin density at the abstracting, preferentially terminal oxygen atom of $M{-}O_t^{\bullet}$ is crucial.
2) Cationic systems are generally more reactive than neutral or anionic analogues.

© 2015 Wiley-VCH Verlag GmbH & Co. KGaA, Weinheim

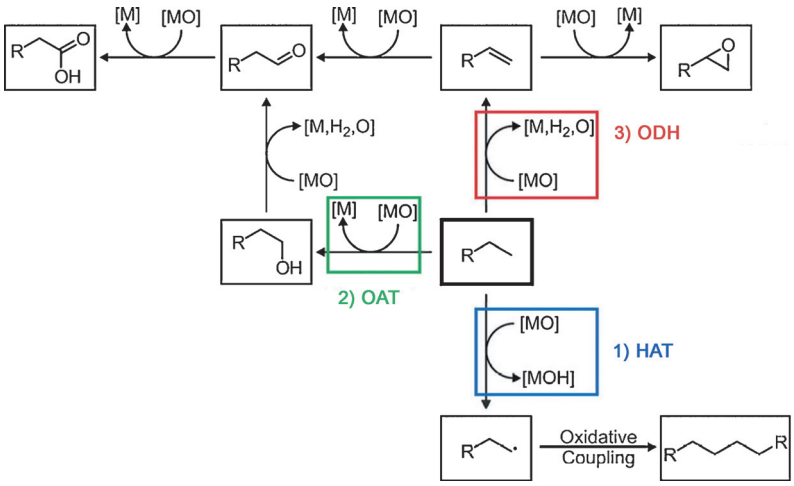

Figure 10. Schematic description of three metal-oxide-mediated oxidation processes of hydrocarbons, all commencing with C–H bond activation: hydrogen-atom transfer (HAT), oxygen-atom transfer (OAT), and oxidative dehydrogenation (ODH; adapted from Ref. [81]).

3) Depending on the nature of the metal-oxide clusters two mechanistic scenarios exist. The direct HAT process prevails predominantly for open-shell oxide clusters with metal centers in relatively high oxidation states and with coordination numbers that prevent interaction of RH with the metal center. A canonical, well studied system is $[V_4O_{10}]^{\bullet+}/CH_4$.[85] The indirect, metal-mediated pathway is generally limited to small, diatomic metal oxides having vacant sites to permit prior coordination of RH to the metal; here, the metal keeps control of the fate of RH from its initial coordination through C–H bond scission to the eventual liberation of R$^{\bullet}$. For both scenarios there exist numerous examples,[68] and a more recent, rather intriguing one for the indirect process corresponds to the couple $[CuO]^+/CH_4$.[86]

While these general reactivity patterns pertain to both homo- and heteronuclear cluster oxides, the latter systems permit to modify crucial properties, for example, spin densities or local charge distributions around the reaction centers by judicious choices of the dopants. As a good example on how the spin density at the H-accepting oxygen atom can be changed by doping, let us discuss the reactivity of $[MgO]_n^{\bullet+}$ ($n = 1$–7) clusters toward hydrocarbons. While diatomic $[MgO]^{\bullet+}$ initiates HAT even from CH_4, the larger clusters with $n \geq 2$ are completely inert toward methane, even though the reactions are exothermic. Why is this so? In contrast to diatomic $[MgO]^{\bullet+}$, in $[Mg_2O_2]^{\bullet+}$ the spin is equally distributed over the two bridging oxygen atoms of the cluster; intracluster spin-density transfer and the associated kinetic barrier for HAT from CH_4 are too high in energy to be accessible under thermal conditions. Thus, HAT is only observed with those substrates that have weaker C–H bonds, as for example, propane or butane.[87,88] However, doping the $[Mg_2O_2]^{\bullet+}$ cluster with Ga_2O_3 changes the reactivity completely, in that C_2H_6 and even CH_4 undergo HAT at room temperature.[89] This is due to the fact that in the $[Ga_2Mg_2O_5]^{\bullet+}$ cluster, the spin density of a bridging O atom at the active site is increased to 0.896 compared to 0.517 on each O atom in $[Mg_2O_2]^{\bullet+}$ and 0.092 at the O atom in the center of $[Ga_2Mg_2O_5]^{\bullet+}$. Also the negative charge around the active site of the heteronuclear cluster is reduced to −0.941 e compared to −1.279 e for $[Mg_2O_2]^{\bullet+}$. As a consequence, the potential-energy surfaces for the HAT reactions are such that activation of RH (R = CH_3, C_2H_5) by $[Ga_2Mg_2O_5]^{\bullet+}$ becomes possible at room temperature (Figure 11).

He and co-workers investigated the effects of the doping-induced local charge distributions around the active O$^{\bullet}$ centers.[69,70,90] As shown in Figure 12, the relative rate constants, krel, for HAT from CH4 correlate very well with the local positive charges (Q_L) around the M–O$^{\bullet}$ centers. Common to all systems in Figure 12 is that the net charge of the cluster ion is +1 and that the clusters contain terminal O$^{\bullet}$ radicals in the active site. Thus, the huge differences in reactivity suggest that changing the charge distribution within

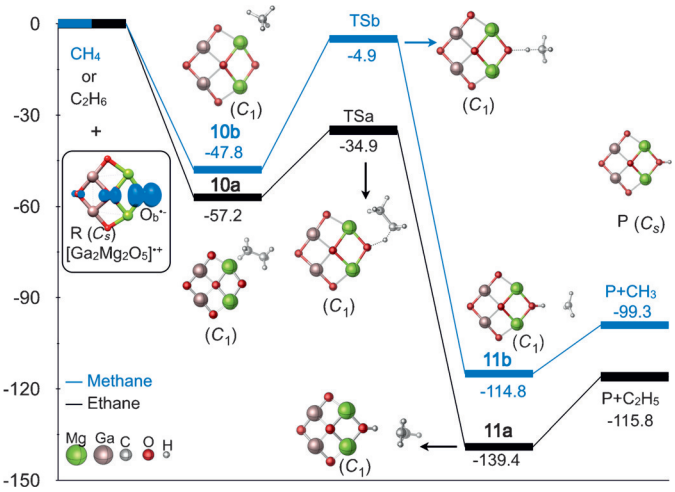

Figure 11. The potential-energy surfaces (kJ mol^{-1}) and key ground-state structures involved in the reactions of $[Ga_2Mg_2O_5]^{\bullet+}$ with a) C_2H_6 and b) CH_4, calculated at the G4MP2-6X level of theory. The inset shows the ground-state structure of $[Ga_2Mg_2O_5]^{\bullet+}$, and the blue isosurfaces indicate the spin-density distributions calculated using the "atoms in molecules" (AIM) approach (adapted from Ref. [89]).

 © 2015 Wiley-VCH Verlag GmbH & Co. KGaA, Weinheim

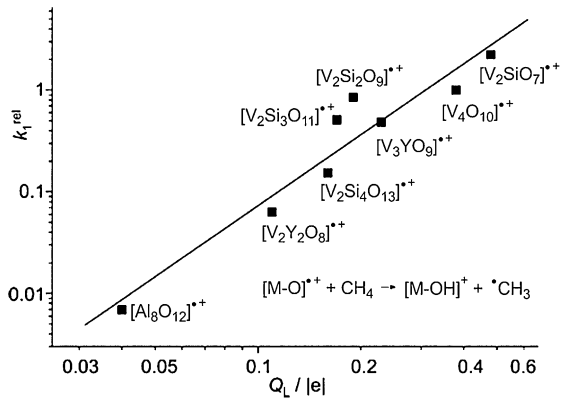

Figure 12. Variation of the experimentally determined relative rate constants (k_{rel}) with respect to the calculated local charges (Q_L) with: $k_{rel} = k_1(X + CH_4)/k_1([V_4O_{10}]^{\bullet+} + CH_4)$; X = $[Al_8O_{12}]^{\bullet+}$; $[V_2O_5(SiO_2)_{1-4}]^{\bullet+}$, and $[V_{4-n}Y_nO_{10-n}]^{\bullet+}$, n = 0–2 (adapted from Ref. [90]).

a small cluster either by doping or, quite interestingly, even by applying external electric fields[91,92] can affect the barriers for HAT significantly.

As already mentioned, the overall charge state of clusters can also matter a lot for HAT processes. This becomes obvious when, for example, the charge and spin distribution of the isoelectronic cluster oxides shown in Figure 13 are compared.[93] All three systems possess a high-spin density at a terminal oxygen atom, thus making them good candidates for thermal HAT. In fact, $[VAlO_4]^{\bullet+}$ accomplishes efficient C–H bond scission of CH_4 at room temperature,[94] in line with the potential energy surface (PES) for the couple

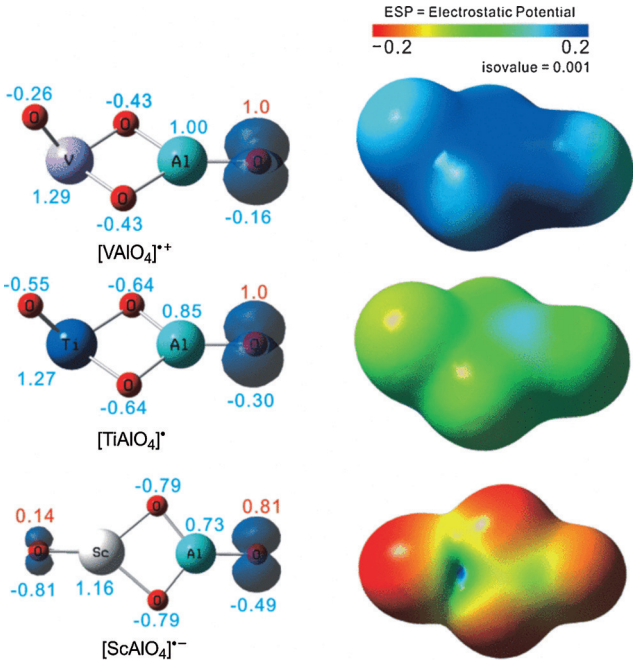

Figure 13. Charge and spin distributions of the isoelectronic clusters $[VAlO_4]^{\bullet+}$, $[TiAlO_4]^{\bullet}$, and $[ScAlO_4]^{\bullet-}$. The Mulliken atomic charge values are denoted in blue and the Mulliken atomic spin distributions are denoted in red on the structures at the left (adapted from Ref. [93]).

$[VAlO_4]^{\bullet+}/CH_4$.[93,94] In contrast, for the structurally related cluster oxides $[TiAlO_4]^{\bullet}$ and $[ScAlO_4]^{\bullet-}$, the PESs clearly indicate barriers along the reaction coordinate, which impede the occurrence of HAT under ambient conditions. Obviously, the approach of the electron-rich hydrocarbon to a negatively charged surface of the metal oxides is not favored.

Gas-phase studies with heteronuclear oxide clusters have also shed light on the role of support materials, for example, phosphates, silicates, and aluminum oxide, in heterogeneous catalysis. These materials are usually considered catalytically innocent linkers between the active metal-oxide sites and the support, as for example in the VPO catalysts, permitting the large-scale transformation of *n*-butane to maleic anhydride.[95] This conjecture was questioned by gas-phase experiments with metal-free oxide clusters; for example, $[P_4O_{10}]^{\bullet+}$ activates methane under ambient conditions with an efficiency of 66% relative to the collision rate.[96] Similarly, oligomeric aluminum oxide clusters $[(Al_2O_3)_n]^{\bullet+}$ (n = 3–5) with an even number of aluminum atoms are capable to activate CH_4 at room temperature.[97] With regard to heteronuclear clusters, for example, $[V_{4-n}P_nO_{10}]^{\bullet+}$,[80] $[(V_2O_5)_n(SiO_2)_m]^{+/-}$ (n = 1, 2; m = 1–4),[98] or $[V_nAl_mO_o]^{+/-}$ ($n+m$ = 2, 3, 4; o = 3–10),[99] they all possess a high spin density located at a terminal oxygen atom that is *not* bound to the transition metal vanadium but to the main-group atom, that is Al–$O_t^{\bullet}$, Si–$O_t^{\bullet}$, or P–$O_t^{\bullet}$. The V=O_t unit is completely inert. Obviously, questions regarding the actual nature of the active site in heteronuclear oxo clusters and the particular role of the various components of a heterogeneous catalyst are once more raised.

3.2 Reactivity Conundrum of the $[V_nP_{4-n}O_{10}]^{\bullet+}/C_2H_x$ Couples (n = 0–4; x = 4, 6)

Common to the thermal reactions of all $[V_nP_{4-n}O_{10}]^{\bullet+}$ clusters with CH_4 is a facile scission of the C–H bond with efficiencies of more than 60% relative to the collision rate.[85,96,100] Also, irrespective of the composition of the cluster, HAT from CH_4 proceeds through a direct pathway, as depicted in Figure 14 exemplarily for the Jahn–Teller-distorted tetrahedral cage structure of $[P_4O_{10}]^{\bullet+}$.[68,96] However, as shown in Table 1, an entirely different scenario is encountered when these cluster ions react with C_2H_x (x = 4, 6),[81,100–102] and the major questions raised by the unexpected branching ratios can be summarized as follows:

1) What are the reasonable reaction mechanisms for these VPO clusters when subjected to these substrates?
2) Why does only the $[V_4O_{10}]^{\bullet+}/C_2H_4$ couple undergo exclusively oxygen-atom transfer, but as soon as one phosphorus atom is present, OAT is no longer observed?
2) Why does the homonuclear cluster $[P_4O_{10}]^{\bullet+}$ not permit the oxidative dehydrogenation (ODH) of the C_2 hydrocarbons?

Clearly, for the reactions of these oxide cluster ions, "composition counts"![3,16,28] Explanations and insight were sought by DFT studies,[81] and here I will only describe part of the results obtained for the $[V_2P_2O_{10}]^{\bullet+}/C_2H_4$ couple.

© 2015 Wiley-VCH Verlag GmbH & Co. KGaA, Weinheim

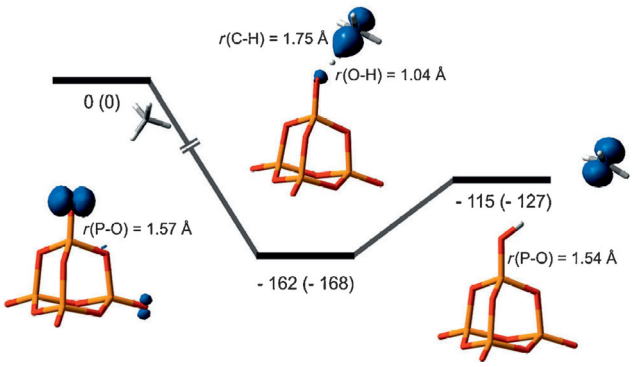

Figure 14. Potential-energy surface for the reaction of $[P_4O_{10}]^{\bullet+}$ with CH_4 (yellow P; red O); the relative energies from DFT and CCSD(T) (in parentheses) are corrected for unscaled zero-point-corrected energies and given in kJ mol^{-1}. Selected bond lengths are given in Å and the blue isosurface indicates the spin density (adapted from Ref. [68]).

Table 1: Branching ratio of the product distributions in the reactions of $[V_nP_{4-n}O_{10}]^{\bullet+}$ ($n=0$, 2–4).[81]

	C_2H_4			C_2H_6		
	OAT	HAT	ODH	OAT	HAT	ODH
$[V_4O_{10}]^{\bullet+}$	100	–	–	–	–	100
$[V_3PO_{10}]^{\bullet+}$	–	36	64	–	79	21
$[V_2P_2O_{10}]^{\bullet+}$	–	38	62	–	83	17
$[P_4O_{10}]^{\bullet+}$	–	100	–	–	100	–

The preference for OAT observed for $[V_4O_{10}]^{\bullet+}/C_2H_4$ and its complete absence for any of the phosphorus-containing systems can be traced back to the bond-dissociation energies (BDEs) for the terminal V–O_t and P–O_t bonds, respectively. As shown in Table 2, BDE(V–O_t) increases when phosphorus

Table 2: BDEs (kJ mol^{-1}) of the terminal V–O_t and P–O_t bonds calculated at the B3LYP/aug-cc-pVTZ//B3LYP/TZVP level of theory.[81]

	$[V_4O_{10}]^{\bullet+}$	$[V_2P_2O_{10}]^{\bullet+}$	$[P_4O_{10}]^{\bullet+}$
BDE(V–O_t)	280	351	–
BDE(P–O_t)	–	396	399

atoms are present in the cluster. In $[V_4O_{10}]^{\bullet+}$, BDE(V–O_t) amounts to only 280 kJ mol^{-1}, which is 71 kJ mol^{-1} lower than the value calculated for $[V_2P_2O_{10}]^{\bullet+}$; in contrast, the BDEs of the terminal P–O bond for the heteronuclear clusters are around 400 kJ mol^{-1}. These features reflect the fact that the ground-state structures of the P-containing cluster oxides possess a P–$O_t^{\bullet}$ bond; a V–$O_t^{\bullet}$ bond is only present in $[V_4O_{10}]^{\bullet+}$. Thus, extra energy in addition to the 280 kJ mol^{-1} is required to cleave an inert V=O bond. While for the heteronuclear clusters the removal of an electron from the P=O rather than from a V=O bond is energetically favored, the resulting BDEs (P–O_t) are still so high that OAT from heteronuclear VPO clusters is energetically prohibited.

The branching ratios of the competing HAT and ODE channels depend on the relative energies required to form the $[V_2P_2O_{10}H]^{+}$ and $[V_2P_2O_{10}H_2]^{\bullet+}$ product ions, respectively. HAT gives rise to a closed-shell product ion concomitant with spin transfer from the cluster to the emerging hydrocarbon radical; in contrast, open-shell systems are regenerated in the course of the second hydrogen-atom transfer, which is accompanied by the reduction of a vanadium or phosphorus atom to the formal oxidation state +IV. As this oxidation state is disfavored for phosphorus, $[P_4O_{10}]^{\bullet+}$ prefers HAT rather than ODH. However, the presence of a redox-active vanadium atom opens up the ODH channel for the heteronuclear oxide cluster.

Quite detailed mechanistic insight has been derived from a DFT analysis (Figure 15).[81] The initially formed encounter complex **13** serves as branching point for two different reaction channels A (OAT) and B (HAT and ODH). In pathway A, which has already been identified by Castleman and co-workers for the $[V_4O_{10}]^{\bullet+}/C_2H_4$ couple,[103] a hydrogen atom from the oxygen-bound methylene group undergoes a 1,2 migration (via **TS 13/14**) to form intermediate **14**.

Remarkable differences among the VPO clusters that were investigated relate to the spin distributions of **TS 13/14** and intermediate **14**. In line with avoiding a high spin density at a P atom and the energetic disadvantage of an associated reduction $P^{+V}\rightarrow P^{+IV}$, the spin in $^{14}\mathbf{P_4}$ (i.e., the all-phosphorus intermediate) is located at the C2-unit and the C–O bond length in the CH_3CHO building block is rather long, amounting to 1.472 Å. This feature makes **TS 13/14** energetically rather unfavorable for the vanadium-free system. For the vanadium-containing species, the bonding situation is quite different: 1) the respective C–O bond length in **14** is around 1.25 Å, and 2) the spin density in **TS 13/14** has been shifted to a vanadium atom of the cluster; thus, for these systems the actual hydrogen migration corresponds to a more favorable 1,2 hydride shift within a cationic, closed-shell C2 unit (Figure 16).

Pathway B results either in HAT or ODH with **16** serving as a common intermediate for both processes. In competition with the evaporation of $C_2H_3^{\bullet}$ to form **17**, the incipient vinyl radical can rebind to the oxygen atom of the newly formed hydroxy group (**16**→**18**). For vanadium-containing systems, the spin density is exclusively located at one of the vanadium atoms within the cluster skeleton, and the reaction continues through the transfer of the C_2H_3 fragment to a bridging, vanadium-bound oxygen atom (**18**→**19**). The ODH process is completed by yet another hydrogen-atom migration from the terminal CH_2 unit to the adjacent V=O site, thus generating **20**, from which C_2H_2 can be liberated. The formal 1,2 elimination in the overall ODH process $C_2H_4\rightarrow C_2H_2+H_2$ has been confirmed by labeling, with $CH_2{=}CD_2$ leading to the specific transfer of HD to the cluster ion.[100]

The reactivity patterns observed in the reactions of the well-studied homonuclear clusters $[V_4O_{10}]^{\bullet+}$ and $[P_4O_{10}]^{\bullet+}$ with C_2H_4 are consistent with the calculated PESs.[81] For $[V_4O_{10}]^{\bullet+}$, OAT is kinetically and thermodynamically clearly favored; the same holds true for the HAT pathway in the case of $[P_4O_{10}]^{\bullet+}$. The branching ratio of OAT versus HAT/ODH is mainly determined by the relative energies of the barriers **TS 13/14** versus **TS 13/16** in Figure 15, respectively. For example, the OAT transition structure **TS 13/14** is energetically lowest for the $[V_4O_{10}]^{\bullet+}/C_2H_4$ couple and increases upon

 © 2015 Wiley-VCH Verlag GmbH & Co. KGaA, Weinheim

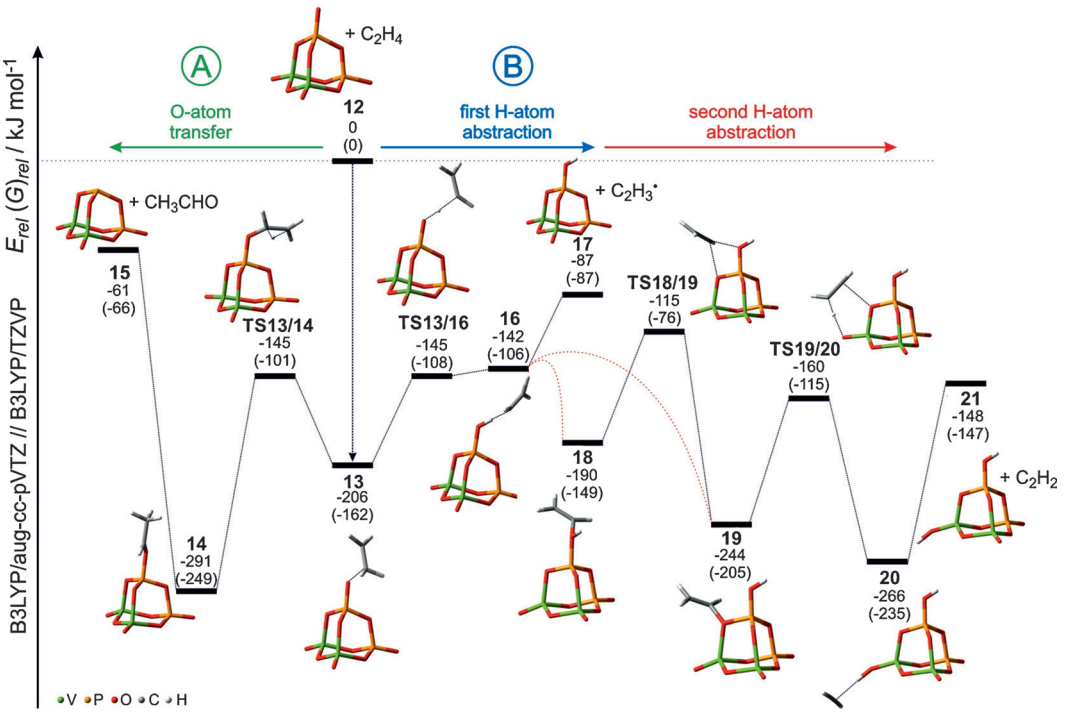

Figure 15. Potential-energy surface (PES) for the reactions of $[V_2P_2O_{10}]^{\bullet+}$ (**12**) with C_2H_4, calculated at B3LYP/aug-cc-pVTZ//B3LYP/TZVP level of theory (green V; yellow P; red O; gray C; white H). The electronic energies and relative Gibbs free energies (in parenthesis) are given in kJ mol^{-1} and corrected for unscaled zero-point energy contributions (adapted from Ref. [81]).

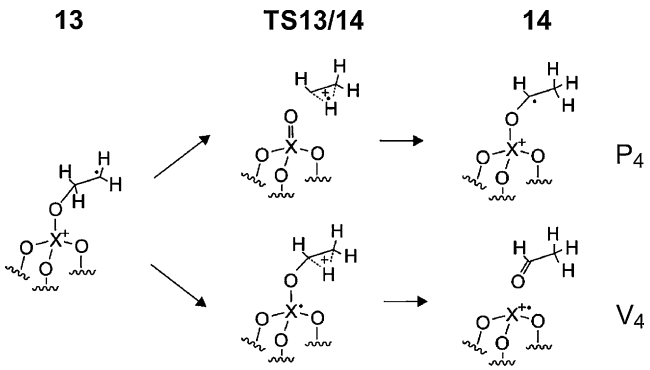

Figure 16. Schematic description of the process **13**→**TS13/14**→**14** for the homonuclear couples $[X_4O_{10}]^{\bullet+}/C_2H_4$ with X = P, V (adapted from Ref. [81]).

doping the cluster with phosphorus atoms. With respect to the HAT channel, the replacement of one vanadium atom by phosphorus has only a minor effect on the relative energy of **TS13/16**. Finally, the non-observation of the second hydrogen-atom transfer in the case of the homonuclear $[P_4O_{10}]^{\bullet+}/C_2H_4$ couple results from the unfavorable energetic situation of the corresponding all-phosporus transition structure **TS19/20**, reflecting the reluctance of phosphorus to attain the formal oxidation state + IV. Quite clearly, the combination of a main-group element (phosphorus) with a transition metal (vanadium) in these structurally related adamantoid heteronuclear cluster oxides gives rise to new product distributions when compared to the homonuclear analogues; furthermore, the heteronuclear clusters illustrate the existence of remarkable co-operative effects between metals and nonmetals in complex oxo frameworks.

4. Conclusions and Prospects

In a superb review on fundamental aspects of gas-phase organometallic chemistry, Armentrout and Beauchamp noted that "… *it remains a source of frustration to know so much about the reactions of transition-metal ions with hydrocarbons and yet have so many questions remain unanswered*".[104] Processes of higher complexity, involving for example "free" clusters were considered as "largely shrouded in mystery".[104] However, over the last few decades things have changed—and, fortunately, to the better! This is in no small part due to breathtaking instrumental developments that permit experiments, which were thought of as simply impossible a quarter of a century ago; also the progress in theoretical chemistry and the introduction of new concepts, for example, the role of electronically excited states in thermal processes,[105] have contributed enormously.

As shown in this Minireview, there is good reason to argue that an integrated experimental/computational approach helps to address important problems that extend well beyond traditional gas-phase chemistry and physics. The study of "doped" cluster oxides enables one to modify in an engineered way features such as the charge and spin states of a reacting system, to identify the active site of a catalyst, to disentangle the role of the support from the active component in composite material, or to affect and control to some extent branching ratios of competing processes.

© 2015 Wiley-VCH Verlag GmbH & Co. KGaA, Weinheim

Finally, there is also hope that quite a few of the mechanistic challenges associated with the activation of small molecules, for example, carbon dioxide, dihydrogen, methane, or water can be addressed at a strictly molecular level. Thus, at long last, bridging the gap between chemistry conducted in the gas phase and the most complex behavior at surfaces or in solution seems possible,[3,8,10,15] provided scientists do not ignore Gerhard Ertl's gentle reminder about the relationship between the simple and the complex (Figure 17).[106]

Figure 17. About the simple and the complex (with courtesy from G. Ertl, Berlin). The text reads "A baguette is more than the sum of its crumbs".

This work is supported by the Deutsche Forschungsgemeinschaft and the Fonds der Chemischen Industrie. Technical assistance in the preparation of the manuscript by Andrea Beck, Dr. Maria Schlangen-Ahl, and Dr. Nicole Rijs is appreciated. I am particularly grateful for the conceptual, intellectual, and practical contributions of present and past coworkers, as well as for encouragement by fellow colleagues.

How to cite: *Angew. Chem. Int. Ed.* **2015**, *54*, 10090–10100
Angew. Chem. **2015**, *127*, 10228–10239

[1] X.-F. Yang, A. Wang, B. Qiao, J. Li, J. Liu, T. Zhang, *Acc. Chem. Res.* **2013**, *46*, 1740.
[2] R. A. J. O'Hair, G. N. Khairalla, *J. Cluster Sci.* **2004**, *15*, 331.
[3] D. K. Böhme, H. Schwarz, *Angew. Chem. Int. Ed.* **2005**, *44*, 2336; *Angew. Chem.* **2005**, *117*, 2388.
[4] S. Yin, E. R. Bernstein, *Int. J. Mass Spectrom.* **2012**, *321*, 49.
[5] M. Schlangen, H. Schwarz, *Catal. Lett.* **2012**, *142*, 1265.
[6] G. Ertl, T. Gloyna, *Z. Phys. Chem. (Muenchen Ger.)* **2003**, *217*, 1207.
[7] J.-M. Thomas, R. Raja, D. W. Lewis, *Angew. Chem. Int. Ed.* **2005**, *44*, 6456; *Angew. Chem.* **2005**, *117*, 6614.
[8] G. Ertl, *Angew. Chem. Int. Ed.* **2008**, *47*, 3524; *Angew. Chem.* **2008**, *120*, 3578.
[9] H. Schwarz, *Isr. J. Chem.* **2014**, *54*, 1413.
[10] S. M. Lang, T. M. Bernhardt, *Phys. Chem. Chem. Phys.* **2012**, *14*, 9255.
[11] M. Diefenbach, M. Brönstrup, M. Aschi, D. Schröder, H. Schwarz, *J. Am. Chem. Soc.* **1999**, *121*, 10614.
[12] K. Koszinowski, D. Schröder, H. Schwarz, *Organometallics* **2004**, *23*, 1132.
[13] R. Horn, G. Meste, M. Thiede, F. C. Jentoft, P. M. Schmidt, M. Bewersdorf, R. Weber, R. Schlögl, *Phys. Chem. Chem. Phys.* **2004**, *6*, 4514.
[14] G. E. Johnson, R. Mitrić, V. Bonačić-Koutecký, A. W. Castleman Jr., *Chem. Phys. Lett.* **2009**, *475*, 1.
[15] J. Sauer, H.-J. Freund, *Catal. Lett.* **2015**, *145*, 109.
[16] A. W. Castleman Jr., K. H. Bowen, *J. Phys. Chem.* **1996**, *100*, 12911.
[17] R. Ferrando, J. Jellinek, R. L. Johnston, *Chem. Rev.* **2008**, *108*, 845.
[18] B. Qiao, A. Wang, X. Yang, L. F. Allard, Z. Jiang, Y. Ciu, J. Liu, J. Li, T. Zhang, *Nat. Chem.* **2011**, *3*, 634.
[19] M. Behrens, F. Studt, I. Kasatkin, S. Kühl, M. Hävecker, F. Abild-Petersen, S. Zander, F. Girgsdies, P. Jurr, B.-L. Kniep, M. Tovar, R. W. Fischer, J. K. Nørskov, R. Schlögl, *Science* **2012**, *336*, 893.
[20] J.-F. Wu, S.-M. Yu, W. D. Wang, Y.-X. Fan, S. Bai, C.-H. Zhang, Q. Gao, J. Huang, W. Wang, *J. Am. Chem. Soc.* **2013**, *135*, 13567.
[21] J. K. Edwards, G. J. Hutchings, *Angew. Chem. Int. Ed.* **2008**, *47*, 9192; *Angew. Chem.* **2008**, *120*, 9332.
[22] X. Zhang, G. Liu, G. Ganteför, K. H. Bowen, A. N. Alexandrova, *J. Phys. Chem. Lett.* **2014**, *5*, 1596.
[23] J.-H. Meng, S.-G. He, *J. Phys. Chem. Lett.* **2014**, *5*, 3890.
[24] C. Heinemann, H. H. Cornehl, D. Schröder, M. Dolg, H. Schwarz, *Inorg. Chem.* **1996**, *35*, 2463.
[25] H. Schwarz, *Angew. Chem. Int. Ed.* **2011**, *50*, 10096; *Angew. Chem.* **2011**, *123*, 10276.
[26] V. J. F. Lapoutre, B. Redlich, A. F. G. van der Meer, J. Oomens, J. M. Bakker, A. Sweeney, A. Mookherjee, P. B. Armentrout, *J. Phys. Chem. A* **2013**, *117*, 4115.
[27] K. Koszinowski, D. Schröder, H. Schwarz, *J. Am. Chem. Soc.* **2003**, *125*, 3676.
[28] K. Koszinowski, D. Schröder, H. Schwarz, *ChemPhysChem* **2003**, *4*, 1233.
[29] K. Koszinowski, D. Schröder, H. Schwarz, *Organometallics* **2003**, *22*, 3809.
[30] K. Koszinowski, D. Schröder, H. Schwarz, *Angew. Chem. Int. Ed.* **2004**, *43*, 121; *Angew. Chem.* **2004**, *116*, 124.
[31] F. Xia, J. Chen, Z. Cao, *Chem. Phys. Lett.* **2006**, *418*, 386.
[32] L. Jiang, T. Wende, P. Claes, S. Bhattacharyya, M. Sierka, G. Meijer, P. Lievens, J. Sauer, K. Asmis, *J. Phys. Chem. A* **2011**, *115*, 11187.
[33] K. R. Asmis, *Phys. Chem. Chem. Phys.* **2012**, *14*, 9270.
[34] B. Helmich, M. Sierka, J. Döbler, J. Sauer, *Phys. Chem. Chem. Phys.* **2014**, *16*, 8441.
[35] D. J. Harding, A. Fielicke, *Chem. Eur. J.* **2014**, *20*, 3258.
[36] R. Bell, K. A. Zemski, K. P. Kerns, H. T. Deng, A. W. Castleman Jr., *J. Phys. Chem. A* **1998**, *102*, 1733.
[37] N. Dietl, T. Wende, K. Chen, L. Jiang, M. Schlangen, X. Zhang, K. R. Asmis, H. Schwarz, *J. Am. Chem. Soc.* **2013**, *135*, 3711.
[38] K. R. Asmis, G. Meijer, M. Brümmer, C. Kaposta, G. Santambrogio, L. Wöste, J. Sauer, *J. Chem. Phys.* **2004**, *120*, 6461.
[39] H.-J. Freund, G. Meijer, M. Scheffler, R. Schlögl, M. Wolf, *Angew. Chem. Int. Ed.* **2011**, *50*, 10064; *Angew. Chem.* **2011**, *123*, 10242.
[40] Q. Liu, S.-G. He, *Chem. J. Chin. Univ.* **2014**, *35*, 665.
[41] M. Neumaier, F. Weigend, O. Hampe, M. Kappes, *J. Chem. Phys.* **2006**, *125*, 104308–104301.
[42] D. M. Popolan, M. Nößler, R. Mitrić, T. M. Bernhardt, V. Bonačić-Koutecký, *Phys. Chem. Chem. Phys.* **2010**, *12*, 7865.
[43] D. M. Popolan, M. Nössler, R. Mitrić, T. M. Bernhardt, V. Bonačić-Koutecký, *J. Phys. Chem. A* **2011**, *115*, 951.
[44] H. T. Le, S. M. Lang, J. de Haeck, P. Lievens, E. Janssens, *Phys. Chem. Chem. Phys.* **2012**, *14*, 9350.
[45] Z.-C. Wang, N. Dietl, R. Kretschmer, T. Weiske, M. Schlangen, H. Schwarz, *Angew. Chem. Int. Ed.* **2011**, *50*, 12351; *Angew. Chem.* **2011**, *123*, 12559.

© 2015 Wiley-VCH Verlag GmbH & Co. KGaA, Weinheim

[46] G. E. Johnson, E. C. Tyo, A. W. Castleman Jr., *J. Phys. Chem. A* **2008**, *112*, 4732.
[47] J.-B. Ma, Z.-C. Wang, M. Schlangen, S.-G. He, H. Schwarz, *Angew. Chem. Int. Ed.* **2013**, *52*, 1226; *Angew. Chem.* **2013**, *125*, 1264.
[48] W. Lai, C. Lui, H. Chen, S. Shaik, *Angew. Chem. Int. Ed.* **2012**, *51*, 5556; *Angew. Chem.* **2012**, *124*, 5652.
[49] G. E. Johnson, R. Mitrić, E. C. Tyo, V. Bonačić-Koutecký, *J. Am. Chem. Soc.* **2008**, *130*, 13912.
[50] G. E. Johnson, R. Mitrić, M. Nössler, E. C. Tyo, V. Bonačić-Koutecký, A. W. Castleman Jr., *J. Am. Chem. Soc.* **2009**, *131*, 5460.
[51] M. Nößler, R. Mitrić, V. Bonačić-Koutecký, G. E. Johnson, E. C. Tyo, A. W. Castleman Jr., *Angew. Chem. Int. Ed.* **2010**, *49*, 407; *Angew. Chem.* **2010**, *122*, 417.
[52] M. Haruta, N. Yamada, T. Kobayashi, S. Iijima, *J. Catal.* **1989**, *115*, 301.
[53] M. Haruta, *Catal. Today* **1997**, *36*, 153.
[54] Y. D. Kim, *Int. J. Mass Spectrom.* **2004**, *238*, 17.
[55] T. M. Bernhardt, *Int. J. Mass Spectrom.* **2005**, *243*, 1.
[56] Z. Yuan, X.-N. Li, S.-G. He, *J. Phys. Chem. Lett.* **2014**, *5*, 1585.
[57] X.-N. Li, Z. Yuan, S.-G. He, *J. Am. Chem. Soc.* **2014**, *136*, 3617.
[58] Z.-Y. Li, Z. Yuan, X.-N. Li, Y.-X. Zhao, S.-G. He, *J. Am. Chem. Soc.* **2014**, *136*, 14307.
[59] D. Widmann, R. J. Behm, *Angew. Chem. Int. Ed.* **2011**, *50*, 10241; *Angew. Chem.* **2011**, *123*, 10424.
[60] L. Li, A. Wang, B. Qiao, J. Lin, Y. Huang, X. Wang, T. Zhang, *J. Catal.* **2013**, *299*, 90 – 100.
[61] H. Schwarz, *Angew. Chem. Int. Ed.* **2003**, *42*, 4442; *Angew. Chem.* **2003**, *115*, 4580.
[62] P. Pyykkö, *Angew. Chem. Int. Ed.* **2004**, *43*, 4412; *Angew. Chem.* **2004**, *116*, 4512.
[63] D. Schröder, H. Schwarz, *Angew. Chem. Int. Ed. Engl.* **1995**, *34*, 1973; *Angew. Chem.* **1995**, *107*, 2126.
[64] D. Schröder, H. Schwarz, *Proc. Natl. Acad. Sci. USA* **2008**, *105*, 18114.
[65] G. E. Johnson, E. C. Tyo, A. W. Castleman Jr., *Proc. Natl. Acad. Sci. USA* **2008**, *105*, 18108.
[66] M. Schlangen, H. Schwarz, *Dalton Trans.* **2009**, 10155.
[67] J. Roithová, D. Schröder, *Chem. Rev.* **2010**, *110*, 1170.
[68] N. Dietl, M. Schlangen, H. Schwarz, *Angew. Chem. Int. Ed.* **2012**, *51*, 5544; *Angew. Chem.* **2012**, *124*, 5638.
[69] Y.-X. Zhao, X.-N. Wu, J.-B. Ma, S.-G. He, X.-L. Ding, *Phys. Chem. Chem. Phys.* **2011**, *13*, 1925.
[70] X.-L. Ding, X.-N. Wu, Y.-X. Zhao, S.-G. He, *Acc. Chem. Res.* **2012**, *45*, 382.
[71] M. Brönstrup, D. Schröder, I. Kretzschmar, H. Schwarz, J. N. Harvey, *J. Am. Chem. Soc.* **2001**, *123*, 142.
[72] A. Fiedler, I. Kretzschmar, D. Schröder, H. Schwarz, *J. Am. Chem. Soc.* **1996**, *118*, 9941.
[73] Z.-C. Wang, N. Dietl, R. Kretschmer, J.-B. Ma, T. Weiske, M. Schlangen, H. Schwarz, *Angew. Chem. Int. Ed.* **2012**, *51*, 3703; *Angew. Chem.* **2012**, *124*, 3763.
[74] M. K. Beyer, C. B. Berg, V. Bondybey, *Phys. Chem. Chem. Phys.* **2001**, *3*, 1840.
[75] Y.-X. Zhao, X.-N. Wu, Z.-C. Wang, S.-G. He, *Chem. Commun.* **2010**, *46*, 1736.
[76] X.-X. Zhao, X.-L. Ding, Y.-P. Ma, Z.-C. Wang, S.-G. He, *Theor. Chem. Acc.* **2010**, *127*, 449.
[77] J.-B. Ma, Z.-C. Wang, M. Schlangen, S.-G. He, H. Schwarz, *Angew. Chem. Int. Ed.* **2012**, *51*, 5991; *Angew. Chem.* **2012**, *124*, 6093.
[78] a) Y.-X. Zhao, Z.-Y. Li, Z. Yuan, X.-N. Li, S.-G. He, *Angew. Chem. Int. Ed.* **2014**, *53*, 9482; *Angew. Chem.* **2014**, *126*, 9636; b) for the effect of an Au atom in the $[AuNbO_3]^{+\cdot}$ mediated $CH_4 \rightarrow CH_2O$ conversion, see: L. N. Wang, Z.-X. Zhou, X.-N. Li, T.-M. Mei, S.-G. He, *Chem. Eur. J.* **2015**, *21*, 6957.
[79] Z.-C. Wang, T. Weiske, R. Kretschmer, M. Schlangen, M. Kaupp, H. Schwarz, *J. Am. Chem. Soc.* **2011**, *133*, 16930.
[80] L.-H. Tian, T.-M. Ma, X.-N. Li, S.-G. He, *Dalton Trans.* **2013**, *42*, 11205.
[81] N. Dietl, X. Zhang, C. van der Linde, M. K. Beyer, M. Schlangen, H. Schwarz, *Chem. Eur. J.* **2013**, *19*, 3017.
[82] S. Arndt, G. Laugel, S. Levchenko, R. Horn, M. Baerns, M. Scheffler, R. Schlögl, R. Schomäcker, *Catal. Rev.* **2011**, *53*, 424.
[83] K. Kwapien, J. Paier, J. Sauer, M. Geske, U. Zavyalova, R. Horn, P. Schwach, A. Trunschke, R. Schlögl, *Angew. Chem. Int. Ed.* **2014**, *53*, 8774; *Angew. Chem.* **2014**, *126*, 8919.
[84] A. Oda, H. Torigore, A. Itadani, T. Okhubo Yumura, H. Kobayashi, Y. Kuroda, *J. Phys. Chem. C* **2014**, *118*, 15234.
[85] S. Feyel, J. Döbler, D. Schröder, J. Sauer, H. Schwarz, *Angew. Chem. Int. Ed.* **2006**, *45*, 4681; *Angew. Chem.* **2006**, *118*, 4797.
[86] N. Dietl, C. van der Linde, M. Schlangen, M. K. Beyer, H. Schwarz, *Angew. Chem. Int. Ed.* **2011**, *50*, 4966; *Angew. Chem.* **2011**, *123*, 5068.
[87] D. Schröder, J. Roithová, *Angew. Chem. Int. Ed.* **2006**, *45*, 5705; *Angew. Chem.* **2006**, *118*, 5835.
[88] K. Kwapien, M. Sierka, J. Döbler, J. Sauer, M. Haertelt, A. Fielicke, G. Meijer, *Angew. Chem. Int. Ed.* **2011**, *50*, 1716; *Angew. Chem.* **2011**, *123*, 1754.
[89] J. Li, X.-N. Wu, M. Schlangen, S. Zhou, P. González-Navarrete, S. Tang, H. Schwarz, *Angew. Chem. Int. Ed.* **2015**, *54*, 5074; *Angew. Chem.* **2015**, *127*, 5163.
[90] Z.-Y. Li, Y.-X. Zhao, X.-N. Wu, X.-L. Ding, S.-G. He, *Chem. Eur. J.* **2011**, *17*, 11728.
[91] W. Liu, Y. Zhao, R. Zhang, Y. Li, E. J. Lavernia, Q. Jiang, *ChemPhysChem* **2009**, *10*, 3295.
[92] H. Hirao, H. Chen, M. A. Carvajal, Y. Wang, S. Shaik, *J. Am. Chem. Soc.* **2008**, *130*, 3319.
[93] Z.-C. Wang, S. Yin, E. R. Bernstein, *J. Chem. Phys.* **2013**, *139*, 194313 – 194311.
[94] Z.-C. Wang, X.-N. Wu, Y.-X. Zhao, J.-B. Ma, X.-L. Ding, S.-G. He, *Chem. Phys. Lett.* **2010**, *489*, 25.
[95] K. Kourtakis, L. Wang, E. Thompson, P. L. Gai, *Appl. Catal. A* **2010**, *376*, 40.
[96] N. Dietl, M. Engeser, H. Schwarz, *Angew. Chem. Int. Ed.* **2009**, *48*, 4861; *Angew. Chem.* **2009**, *121*, 4955.
[97] S. Feyel, J. Döbler, R. Höckendorf, M. K. Beyer, J. Sauer, H. Schwarz, *Angew. Chem. Int. Ed.* **2008**, *47*, 1946; *Angew. Chem.* **2008**, *120*, 1972.
[98] X.-L. Ding, Y.-X. Zhao, X.-N. Wu, Z.-C. Wang, J.-B. Ma, S.-G. He, *Chem. Eur. J.* **2010**, *16*, 11463.
[99] Z.-C. Wang, X.-N. Wu, Y.-X. Zhao, J.-B. Ma, X.-L. Ding, S.-G. He, *Chem. Eur. J.* **2011**, *17*, 3449.
[100] N. Dietl, R. F. Höckendorf, M. Schlangen, M. Lerch, M. K. Beyer, H. Schwarz, *Angew. Chem. Int. Ed.* **2011**, *50*, 1430; *Angew. Chem.* **2011**, *123*, 1466.
[101] N. Dietl, M. Engeser, H. Schwarz, *Chem. Eur. J.* **2009**, *15*, 11100.
[102] N. Dietl, M. Engeser, H. Schwarz, *Chem. Eur. J.* **2010**, *16*, 4452.
[103] D. R. Justes, R. Mitrić, N. A. Moore, V. Bonačić-Koutecký, W. A. Castleman Jr., *J. Am. Chem. Soc.* **2003**, *125*, 6289.
[104] P. B. Armentrout, J. L. Beauchamp, *Acc. Chem. Res.* **1989**, *22*, 315.
[105] D. Schröder, S. Shaik, H. Schwarz, *Acc. Chem. Res.* **2000**, *33*, 139.
[106] G. Ertl, *Bohlmann Lecture*, Technische Universität Berlin, December 4, 2009.

Received: January 23, 2015
Published online: June 18, 2015

© 2015 Wiley-VCH Verlag GmbH & Co. KGaA, Weinheim